IOP PUBLISHING JOURNAL OF PHYSICS: CONDENSED MATTER
J. Phys.: Condens. Matter **24** (2012) 505501 (7pp) doi:10.1088/0953-8984/24/50/505501

Magnetic properties of Mn-doped Ge_{46} and Ba_8Ge_{46} clathrates

Nirmal Ganguli[1,2], K V Shanavas[3,5] and Indra Dasgupta[1,4]

[1] Department of Solid State Physics, Indian Association for the Cultivation of Science, Jadavpur, Kolkata 700032, India
[2] Department of Physics, Indian Institute of Technology Bombay, Mumbai 400076, India
[3] High Pressure and Synchrotron Radiation Physics Division, BARC, Mumbai 400085, India
[4] Center for Advanced Materials, Indian Association for the Cultivation of Science, Jadavpur, Kolkata 700032, India

E-mail: sspid@iacs.res.in (I Dasgupta)

Received 24 July 2012, in final form 3 October 2012
Published 19 November 2012
Online at stacks.iop.org/JPhysCM/24/505501

Abstract
We present a detailed study of the magnetic properties of unique cluster assembled solids, namely Mn-doped Ge_{46} and Ba_8Ge_{46} clathrates using density functional theory. We find that ferromagnetic ground states may be realized in both compounds when doped with Mn. In Mn_2Ge_{44}, ferromagnetism is driven by hybridization-induced negative exchange splitting, a generic mechanism operating in many diluted magnetic semiconductors. However, for Mn-doped Ba_8Ge_{46} clathrates incorporation of conduction electrons via Ba encapsulation results in RKKY-like magnetic interactions between the Mn ions. We show that our results are consistent with the major experimental observations for this system.

(Some figures may appear in colour only in the online journal)

1. Introduction

Cluster assembled solids formed by large cages of Si and Ge, the so-called clathrates, have received considerable attention in recent years because of the wealth of physical properties displayed by them. These periodic arrangements of nano-sized cages may be semiconducting with an energy gap larger than that of the standard diamond form of Si and Ge [1]. Alkali/alkaline earth encapsulated Si and Ge clathrates are metals [2]. Some of them are found to be superconducting [3] and are also suggested to be excellent candidates for thermoelectric applications [4]. Efficient storage of hydrogen was also reported in some clathrates [5]. Interestingly, the germanium clathrates were also found to be ferromagnetic upon doping with transition metals (TMs) [6, 7]. Kawaguchi *et al* have reported ferromagnetism in Mn-doped Ba_8Ge_{46} clathrates [6], followed by another report by Li *et al* on ferromagnetism in Fe-doped Ba_6Ge_{25} clathrates [7]. Ferromagnetism was also reported in $Eu_4Sr_4Ga_{16}Ge_{30}$ [8] and $Eu_8Ga_{16}Ge_{30}$ [9] clathrates. The discovery of magnetism in Ge-based clathrates has added a novel functionality to these cluster assembled solids that may find possible application in magnetic devices.

Ge_{46} is a type I clathrate with a simple cubic lattice, where the Ge atoms form closed cage-like structures of Ge_{20} and Ge_{24}. The unit cell consists of two 20-atom (Ge_{20}) cages and six 24-atom (Ge_{24}) cages. Among the two Ge_{20} cages one is placed at the corner of the cube, while the other, rotated 90° with respect to the first, is placed at the body center of the cube. Each Ge in the Ge_{20} cage is bonded to three other atoms within the same cage. The four-fold co-ordination is completed in two steps. The eight Ge atoms in each Ge_{20} cage form bonds along the eight ⟨111⟩ directions with the other Ge_{20} unit and the four-fold co-ordination of the remaining 12 atoms in each Ge_{20} cage is taken care of by adding six Ge atoms at the interstitial 6c sites in the primitive unit cell. In this process all the six Ge atoms added at the 6c sites also become four-fold co-ordinated and generate per Ge_{20} three Ge_{24} cages, which fill the space not occupied by the Ge_{20}

[5] Present address: Department of Physics, University of Missouri, Columbia, MO 65211, USA.

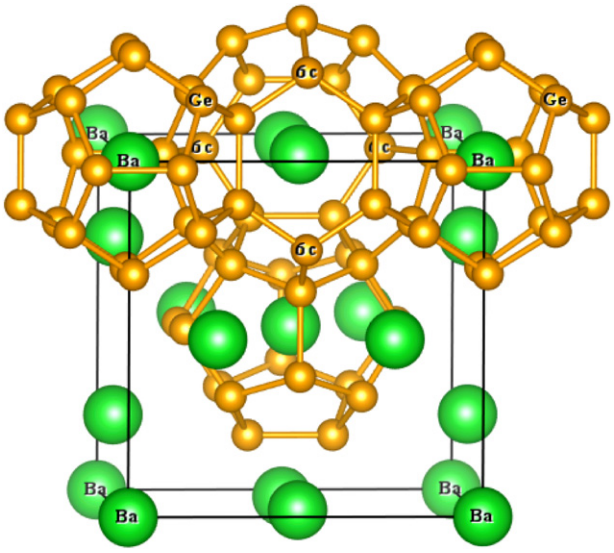

Figure 1. Structure of Ba_8Ge_{46} clathrate showing the simple cubic lattice with Ge_{20} and Ge_{24} cages. Ge atoms at the crystallographic 6c sites are highlighted. All the Ge atoms in the unit cell are not shown for clarity.

cages. The resulting primitive unit cell has two Ge_{20} + six Ge atoms at the 6c sites, i.e. 46 Ge atoms (space group $Pm\bar{3}n$) where each Ge is tetrahedrally bonded and one would therefore expect the material to be semiconducting. Although semiconducting pure Ge clathrates can be experimentally synthesized [10], they prefer to encapsulate alkali and alkaline earth metals like Na, K and Ba which occupy the centers of the Ge_{20} and Ge_{24} cages (see figure 1). Such encapsulation induces a transition from semiconducting phase to a metallic phase [11].

The interstitial 6c sites (highlighted in figure 1) are of particular importance, as the doping of Mn atoms randomly at these 6c sites of Ba_8Ge_{46} clathrate was reported to yield ferromagnetism with saturation magnetic moment per Mn atom ∼0.8 μ_B and the ferromagnetic Curie temperature ∼10 K [6]. The distance between the dopant Mn atoms at the 6c sites was also found to be quite large, so it was also speculated [6] that the interaction between the dopants may be Ruderman–Kittel–Kasuya–Yosida (RKKY)-like. Following this report, Yang *et al* [12] investigated this system in the framework of *ab initio* density functional calculations. For a pair of Mn atoms to be substituted at the 6c sites in the unit cell, if the position of one Mn is fixed then the other can occupy any of the remaining five sites. Out of these five neighbors of Mn, one is at a distance $a/2$, referred to as configuration I, while the other four are at a distance $\sqrt{6}a/4$, referred to as configuration II, where a is the lattice constant. The calculation by Yang *et al* in the framework of the local density approximation (LDA) yielded the value of the magnetic moment per Mn atom to be 0.77 μ_B and 0.42 μ_B when the two Mn atoms are doped in configuration I and configuration II, respectively [12]. Although the former value of the magnetic moment agrees well with the experiment the latter value is found to be substantially less. Further, if the exchange interaction is RKKY-like then there is also a possibility of antiferromagnetic (AFM) coupling between a pair of Mn atoms; however, this possibility was not explored by Yang *et al* [12]. Therefore, more careful investigations are necessary to understand the origin of magnetism in Mn-doped Ba_8Ge_{46} clathrates. In this paper we have studied the magnetic properties of Mn-doped Ba_8Ge_{46} clathrate in some detail using *ab initio* density functional calculations. It is interesting to note that recently guest-free Ge clathrates have been synthesized [10] but there are no reports of successfully doping them with transition metals (TM). Doping TM in these wide band gap clathrates will be particularly important in the context of diluted magnetic semiconductors (DMS). In view of the above, we have also investigated Mn-doped in pristine Ge_{46} clathrates and find that they may be ferromagnetic. Our calculations also reveal that the origin of ferromagnetism in a guest-free Mn_2Ge_{44} system is markedly different from metal encapsulated $Ba_8Mn_2Ge_{44}$. The remainder of the paper is organized as follows: the technical details of our computational work are described in section 2. In section 3, we explain the results of our calculations and finally the work is summarized in section 4.

2. Method and details of calculations

The electronic structure and total energy calculations presented in this paper are performed using *ab initio* density functional theory (DFT) as implemented in the Vienna *ab initio* simulation package (VASP) [13, 14]. The electron–ion interaction in the core and valence part are treated within the projector augmented wave (PAW) method [15] along with the plane wave basis set. We have employed the generalized gradient approximation (GGA) due to Perdue–Burke–Ernzerhof (PBE) [16] to treat the exchange and correlation. The localized Mn d states are treated in the framework of the GGA + U method [17], where calculations are done for several values of U in the range 2–7 eV and J = 1 eV. Atomic positions (only the internal co-ordinates) were relaxed to minimize the Hellman–Feynman forces on each atom with the tolerance value of 10^{-2} eV $Å^{-1}$. The optimum values of the energy cutoff and the size of the k-point mesh are found to be 650 eV and 4 × 4 × 4, respectively, and were accordingly employed in our calculation.

The formation energy (FE) [18] of Mn_2Ge_{44} is calculated using the following expression:

$$\mathrm{FE} = E(\mathrm{Mn_2Ge_{44}}) - E(\mathrm{Ge_{46}}) - 2\mu_{\mathrm{Mn}} + 2\mu_{\mathrm{Ge}} \qquad (1)$$

where $E(Mn_2Ge_{44})$ is the total energy of Mn_2Ge_{44} while $E(Ge_{46})$ is the total energy of pristine Ge_{46} clathrate. μ_{Mn} and μ_{Ge} are the chemical potentials of Mn and Ge in some suitable reservoir. A similar expression was used to calculate the FE of $Ba_8Mn_2Ge_{44}$ clathrate.

3. Results and discussions

To begin with we have computed the electronic structure of pristine Ge_{46} and Ba_8Ge_{46} clathrates without doping. Our

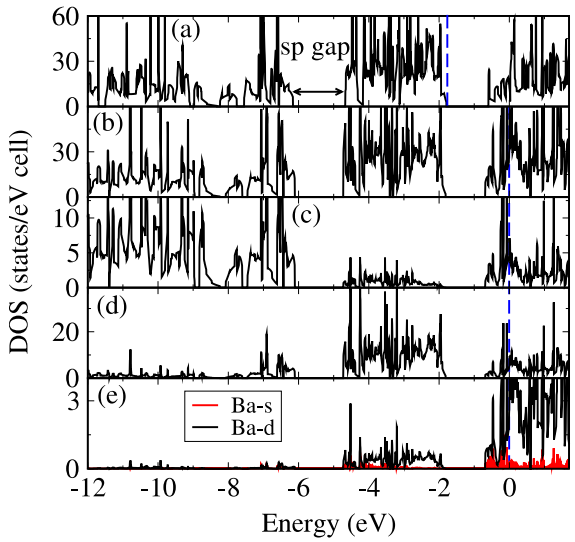

Figure 2. The density of states corresponding to Ge_{46} and Ba_8Ge_{46} clathrates without doping. Part (a) shows the total DOS of Ge_{46} clathrate, while the total DOS of Ba_8Ge_{46} and the partial DOS corresponding to Ge s, Ge p, and Ba s + Ba d states are shown in parts (b)–(e), respectively. The DOS has been plotted by aligning the sp gap in all the panels. The Fermi level is also indicated in each panel.

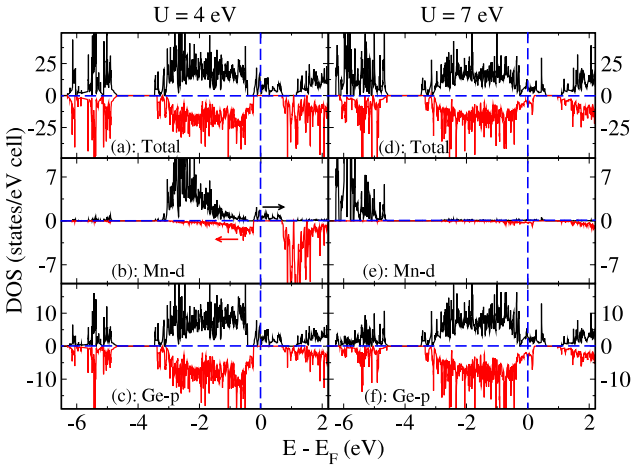

Figure 3. The spin polarized GGA + U ($U = 4$ eV, $J = 1$ eV and $U = 7$ eV, $J = 1$ eV) DOS for Mn_2Ge_{44}, with parallel alignment of Mn spins (FM) in configuration I. Parts (a) and (d) show the total DOS, while (b), (e) and (c), (f) indicate the projected DOS corresponding to Mn 3d and Ge 4p states.

Table 1. Energy difference between antiferromagnetic and ferromagnetic states and the magnetic moments per unit cell (in the ferromagnetic state) for Mn_2Ge_{44} in both configurations and different values of the Hubbard U parameter.

	Configuration I		Configuration II	
U (eV)	$E_{AFM} - E_{FM}$ (meV)	Magnetic moment (μ_B/cell)	$E_{AFM} - E_{FM}$ (meV)	Magnetic moment (μ_B/cell)
0.0	186.3	6.0	151.1	6.0
2.0	182.5	6.0	145.2	6.0
4.0	171.6	6.0	134.3	6.0
5.0	21.5	7.6	14.4	7.7
6.0	10.3	8.2	5.2	8.2
7.0	−6.1	8.5	−8.5	8.7

optimized lattice constants for Ge_{46} and Ba_8Ge_{46} clathrates are 10.78 Å and 11.01 Å, respectively. The density of states corresponding to these clathrates are displayed in figure 2. We see from figure 2(a) that Ge_{46} is a semiconductor with a band gap of 1.19 eV. The gap calculated within the GGA is substantially higher than crystalline Ge in diamond structure, in agreement with earlier results [19]. The valence band density of states (DOS) of the pristine Ge_{46} (figure 2(a), from left to right) exhibits three major parts, as reported earlier [19], that may be assigned to an s-like region, an sp-hybridized region, and a p-like region, with a characteristic s–p gap. The origin of this s–p gap has been attributed to the five ring patterns (pentagons) of the Ge atoms [20]. We have displayed the total as well as the partial DOS for Ba encapsulated Ge_{46} clathrate in figures 2(b) and (c), (d) and (e), respectively. Upon Ba encapsulation the additional 16 valence electrons are accommodated in the conduction band and the system becomes metallic. While the DOS of the valence band of Ba_8Ge_{46} is very similar to pristine Ge_{46}, the conduction band DOS shows modification upon the inclusion of metal atoms. The partial DOS plot of Ba_8Ge_{46} clathrates (see figures 2(c)–(e)) reveals that the conduction band has considerable admixture of Ge s and p states with Ba s and Ba d states with substantial contribution from the latter. These electrons are expected to be delocalized in the entire system and act as a conduction electron cloud.

Next we have considered doping of a pair of Mn atoms at the 6c sites of the semiconducting pristine Ge_{46} clathrate. We calculated the lattice constant for Ge_{46} clathrate doped with two Mn atoms and found no significant difference from that of the pristine Ge_{46} clathrate. The formation energy of Mn_2Ge_{44} is calculated to be 0.80 eV, indicating that such a system may be stable. In order to understand the magnetic properties of the doped system we have calculated the magnetic exchange interactions as the energy difference between antiparallel (AFM) and parallel (FM) arrangements of the magnetic moments of a pair of Mn ions for configurations I and II for several values of U ranging from $U = 0$ (GGA) to $U = 7$ eV. The results of our calculations are displayed in table 1. Our calculations reveal that the exchange interaction is always ferromagnetic in both configurations for all values of U except for $U = 7.0$ eV. These results suggest that Mn-doped Ge_{46} may be ferromagnetic. For further insights on the origin of magnetic ordering in Mn_2Ge_{44} we have displayed in figure 3 the spin polarized DOS for Mn_2Ge_{44} with parallel alignment of the Mn spins (FM) in configuration I for two representative cases, $U = 4$ eV, $J = 1$ eV and $U = 7$ eV, $J = 1$ eV. The DOS for $U = 4$ eV (see figure 3(a)) indicates that the system is a half-metallic ferromagnet, analogous to DMS materials like Mn-doped GaAs. When a Ge is substituted by Mn having seven valence electrons, it is expected that four Mn electrons will be utilized to saturate the Ge dangling bonds and the remaining three electrons will be responsible for

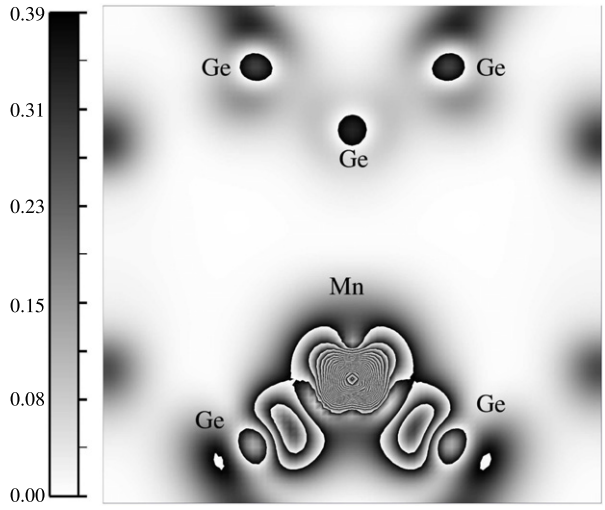

Figure 4. The charge density corresponding to the valence band hole states in the spin up channel for Mn_2Ge_{44}.

the magnetism. A comparison of the total DOS (figure 3(a)) and the projected DOS for Mn d (figure 3(b)) and Ge p (figure 3(c)), however, suggests that the Mn d states are not only strongly exchange split but also Mn d spin up states are fully occupied and the Mn d spin down states are completely empty, confirming that Mn is in high spin d^5 (Mn^{2+}) configuration. So the introduction of Mn in pristine Ge_{46} gives rise to an acceptor in the Ge p manifold and the hole produced by the acceptor (see figure 3(b)) is expected to interact with the localized Mn d states to mediate ferromagnetism. We find from figure 3(b) that the exchange split Mn 3d states in the ferromagnetic configuration strongly hybridizes with the Ge p states. As a result, the spin up Ge p bands shift to higher energy while the spin down Ge p bands make an opposite shift, as indicated by the arrows in figure 3(b). The Fermi level lies in the spin up p-band and therefore an energy gain is obtained by transferring electrons from the Ge spin up states to the Ge spin down ones. The exchange splitting of the p states induced by this hybridization is opposite to that of the Mn d states (i.e. hybridization induced negative exchange splitting). In fact, our calculations reveal that Ge atoms are spin polarized and the magnetic moments of Mn and Ge are oppositely aligned, resulting in the total magnetic moment for the present case to be 6 μ_B per unit cell. This generic mechanism is responsible for ferromagnetism in Sr_2FeMoO_6 [21–23] and Mn-doped GaAs [24] as is further corroborated by the charge density plot of the valence band hole states in the spin up channel, along the (001) plane in an energy window 0.0–0.6 eV relative to the Fermi level shown in figure 4. From this plot we gather that there is strong hybridization of the Mn d states with the Ge p states, thereby accounting for ferromagnetism in Mn-doped Ge_{46}. In the presence of strong hybridization between the Mn d and Ge p states this novel mechanism of ferromagnetism underscores the competing antiferromagnetic ordering of Mn spins via super exchange.

The competition between the ferromagnetism due to hybridization induced negative exchange splitting and antiferromagnetism due to super exchange is controlled by the Hubbard U. The essential role of the Hubbard U is to enhance the exchange splitting of the Mn d states. This is clearly reflected in the plot of the DOS for $U = 7$ eV, $J = 1$ eV as shown in figures 3(d) and (e). So, upon increasing the Hubbard U, the hybridization between the Mn d and Ge p states allowed in the FM configuration of Mn ions is reduced, resulting in very weak exchange splitting of the Ge p states (see figure 3(f)) and the system being metallic. As a consequence there is enhancement of the total magnetic moment as the oppositely aligned Ge moments are small and hardly contribute to the total magnetic moment (see table 1). For a large enough value of U (e.g. $U = 7$ eV), the AFM ordering via super exchange dominates, as can be seen in table 1. However, it is very unlikely that the Hubbard U for Mn in Mn_2Ge_{44} will be large as it will be effectively screened by the Ge s and p electrons and therefore it is expected that Mn_2Ge_{44} will stabilize in the ferromagnetic state.

Table 2. Energy difference between antiferromagnetic and ferromagnetic states and the magnetic moments per unit cell (in the ferromagnetic state) for $Ba_8Mn_2Ge_{44}$ in both configurations and different values of Hubbard U parameter.

	Configuration I		Configuration II	
U (eV)	$E_{AFM} - E_{FM}$ (meV)	Magnetic moment (μ_B/cell)	$E_{AFM} - E_{FM}$(meV)	Magnetic moment (μ_B/cell)
0.0	−22.8	6.1	22.7	6.1
4.0	−54.2	6.3	19.9	6.4
5.0	−56.4	7.5	12.2	7.6
7.0	−142.0	9.1	9.3	9.2

Finally we have considered the doping of Mn in Ba_8Ge_{46}. In our calculations, we have first assumed substitutional doping of two Mn atoms into the Ba_8Ge_{46} clathrate at the 6c sites. The formation energy is calculated to be −6.46 eV, indicating that the system is indeed stable. The equilibrium lattice constant and the atomic positions are calculated for the Mn doped at the 6c sites both in configuration I and configuration II for the ferromagnetic and antiferromagnetic alignment of Mn spins. The equilibrium lattice constant is calculated to be 11.08 Å, which is an overestimation from the experimentally reported value by 3.6%, possibly due to the use of GGA for the exchange–correlation [19]. We have also calculated the electronic structure, the exchange interaction and the magnetic moment per unit cell (in the FM state) in configuration I and configuration II for values of U ranging from $U = 0$ (GGA) to $U = 7$ eV and the results of our calculation are shown in table 2.

We find that in configuration I the exchange interaction is antiferromagnetic while in the configuration II it is ferromagnetic, independent of the chosen values of U (see table 2). This is in sharp contrast to the case of Mn-doped Ge_{46} (see table 1). In order to obtain further insights into the electronic structure we have displayed in figure 5 a plot of the DOS of $Ba_8Mn_2Ge_{44}$ for the representative case $U = 4$ eV and $J = 1$ eV with parallel alignment of Mn spins (FM) in configuration II. The DOS reveals that the

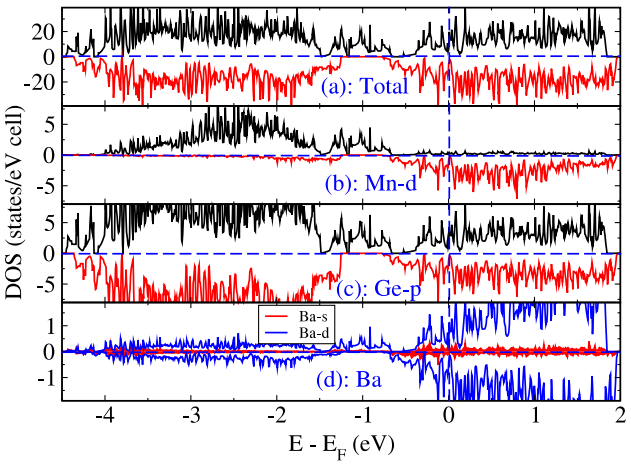

Figure 5. The density of states for parallel alignment of Mn spins (FM) in configuration II for $Ba_8Mn_2Ge_{44}$ clathrate. Part (a) shows the total DOS while the partial DOS corresponding to Mn d, Ge p, and Ba s + Ba d states are shown in parts (b)–(d) respectively.

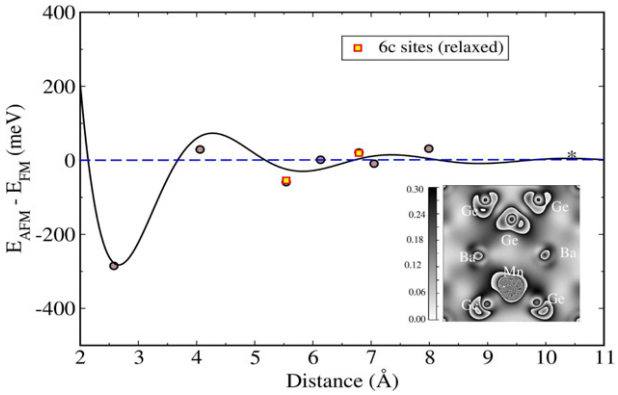

Figure 6. The variation of magnetic exchange interaction strength with distance between the Mn atoms has been plotted and fitted to the RKKY expression with $k_F = 1.05$ Å^{-1}. The inset shows the two-dimensional charge density plot on a plane containing one dopant Mn atom.

Table 3. The relative energies for the Ba_8Ge_{46} system doped with a pair of Mn atoms at different distances in ferromagnetic and antiferromagnetic states. The difference in energy for ferromagnetic and antiferromagnetic states are given in the last column. The energy differences for the relaxed structures are given in parenthesis when Mn atoms are doped at 6c sites.

Mn–Mn distance (Å)	E_{FM} (meV)	E_{AFM} (meV)	$E_{AFM} - E_{FM}$ (meV)
2.58	1168.5	883.3	−285.2
4.06	205.2	234.5	29.3
5.54 (6c)	58.9	0.0	−58.9 (−54.2)
6.13	161.6	163.2	1.6
6.79 (6c)	42.2	63.5	21.3 (19.9)
7.05	276.1	267.1	−9.0
7.99	282.7	314.2	31.5

system is metallic. In comparison to the LDA results [12], in our GGA calculations the exchange splitting underscores the crystal field splitting for the Mn d states. The crystal field splitting is relatively weak in the GGA calculations as the optimized GGA lattice constant is large compared to the LDA calculations and is in better agreement with the experiment. As a consequence, the projected DOS for the Mn d states (figure 5(b) exhibit strong exchange splitting in the Mn d manifold, where the Mn spin up states are completely occupied and as expected the remaining Mn valence electrons are accommodated in the Mn spin down channel accounting for the magnetic moment $\simeq 3\mu_B$/Mn calculated for this system in agreement with the d^7 configuration of Mn. The Fermi level is dominated by the extended Ba s and Ba d states admixed with the Ge s and Ge p states, producing the conduction electron cloud responsible for mediating the exchange interaction.

The metallic state as well as the nature of the exchange interaction, i.e. the change of the magnitude as well as the sign of the exchange interaction with distance, points to the fact that the RKKY model may be applicable here. It is well known that for a fixed concentration of magnetic ions, the RKKY interaction depends only on the distance between the magnetic ions in the presence of the delocalized conduction electron cloud. So in order to extract the characteristic distance dependence of the RKKY exchange interaction, we have also considered in our calculations doping configurations where one Mn is at the 6c site but the second one is either in a 6c site or in other possible framework sites in the unit cell. Such a consideration in our theoretical calculation is based on the fact that the conduction electron cloud spreading over the entire clathrate network mediating the exchange interaction will possibly not distinguish among the three different framework sites. The results of our calculations for the energetics and magnetism for doping a pair of Mn at the 6c sites as well as other sites in the unit cell in Ba_8Ge_{46} for the case $U = 4.0$ eV and $J = 1.0$ eV are summarized in table 3. As expected for the RKKY-like interaction the exchange interaction changes sign as well as magnitude as a function of separation between a pair of Mn ions.

We have fitted the calculated exchange interactions with the RKKY expression for the exchange interaction strength $J(r)$ given by

$$J(r) = \text{Const.}[\sin(2k_F r) - 2k_F r\cos(2k_F r)]/r^4, \qquad (2)$$

where r is the distance between dopant magnetic atoms and k_F is the Fermi wavevector corresponding to the average electron density [25]. Figure 6 shows excellent agreement of the fit with the RKKY model with the fitting parameter $k_F = 1.05$ Å^{-1}, confirming the RKKY mechanism to be operative in Mn-doped Ba_8Ge_{46} clathrates. Further, the plot of the charge density in an energy window −1.2 to −0.6 eV relative to the Fermi level shown in figure 6 (inset) reveals that it is delocalized in the entire system and the exchange interaction is mediated by the conduction electron cloud.

We shall now compare our calculated results with the available experimental data. In view of the large average distance (d) between Mn atoms located at the 6c sites (d = 8.5 Å for lattice constant $a = 10.689$ Å) reported for this

system [6] we have extrapolated the RKKY plot to obtain the exchange interaction between the Mn ions located at the 6c sites other than configuration I and configuration II. For our theoretically calculated lattice constant ($a = 11.08$ Å) the nearest neighbor (configuration I), next nearest neighbor (configuration II) and the third nearest neighbor distances between a pair of Mn atoms occupying the 6c sites are 5.54 Å, 6.79 Å and 10.36 Å, respectively. The RKKY plot reveals that while the nearest neighbor exchange interaction is antiferromagnetic, the next nearest neighbor as well as the third nearest neighbor exchange interactions are ferromagnetic. The large interval among the Mn atoms reported in the experimental work [6] possibly refers to the latter two configurations where the exchange interaction is always ferromagnetic. The small saturation moment (0.8 μ_B) obtained experimentally also finds a natural explanation in such a RKKY scenario. In view of high growth/annealing temperature during synthesis in the radiofrequency induction furnace, the Mn locations are random due to competitive total energies (either ferromagnetic or antiferromagnetic) and the Mn atoms that prefer the antiferromagnetic state do not contribute to the magnetic moment and the moment is due to a small fraction of Mn atoms that are magnetically active in the ferromagnetic state. We also note that the ferromagnetic exchange interaction is very weak (see table 3) for Mn-doped Ba_8Ge_{46} and an estimate of the ferromagnetic transition temperature (T_C) based on RKKY interaction [26] yields a value 6.3 K, in good agreement with experiment [6].

4. Conclusion

In conclusion, we have studied the electronic structure of Ge_{46} and Ba_8Ge_{46} clathrates doped with Mn from *ab initio* density functional calculations. We find that a ferromagnetic ground state may be realized in both the compounds. The origin of ferromagnetism in Mn_2Ge_{44} is driven by hybridization induced negative exchange splitting, a generic mechanism operative in many DMS systems. However, Mn-doped Ba_8Ge_{46} results in RKKY-like magnetic interaction. The origin of the two different mechanism may be traced back to the electronic structure of these systems and the limit of validity of the RKKY model. The RKKY limit, $\frac{E_x}{E_F} \ll 1$, where E_x is the exchange splitting of the host band and E_F is the Fermi energy, is not satisfied for the half-metallic system Mn_2Ge_{44} due to complete spin polarization, resulting in $E_x > E_F$ [24]. However, incorporation of the conduction electrons in $Ba_8Mn_2Ge_{44}$ upon Ba encapsulation makes the system metallic and protects the RKKY limit. The RKKY-like scenario predicted for $Ba_8Mn_2Ge_{44}$ is also consistent with the major experimental observations for this system.

Acknowledgment

The authors acknowledge financial support from DST India (no. INT/EC/MONAMI/(28)/233513/2008).

References

[1] Adams G B, O'Keeffe M, Demkov A A, Sankey O F and Huang Y-M 1994 Wide-band-gap Si in open fourfold-coordinated clathrate structures *Phys. Rev.* B **49** 8048

[2] Moriguchi K, Yonemura M, Shintani A and Yamanaka S 2000 Electronic structures of Na_8Si_{46} and Ba_8Si_{46} *Phys. Rev. B* **61** 9859

[3] Yuan H Q, Grosche F M, Carrillo-Cabrera W, Pacheco V, Sparn G, Baenitz M, Schwarz U, Grin Y and Steglich F 2004 Interplay of superconductivity and structural phase transition in the clathrate Ba_6Ge_{25} *Phys. Rev. B* **70** 174512

[4] Nasir N, Grytsiv A, Melnychenko-Koblyuk N, Rogl P, Bauer E, Lackner R, Royanian E, Giester G and Saccone A 2009 Clathrates $Ba_8\{Zn, Cd\}_xSi_{46-x}$, $x \sim 7$: synthesis, crystal structure and thermoelectric properties *J. Phys.: Condens. Matter* **21** 385404

[5] Neiner D, Okamoto N L, Condron C L, Ramasse Q M, Yu P, Browning N D and Kauzlarich S M 2007 Hydrogen encapsulation in a silicon clathrate type I structure: $Na_{5.5}(H_2)_{2.15}Si_{46}$: synthesis and characterization *J. Am. Chem. Soc.* **129** 13857

[6] Kawaguchi T, Tanigaki K and Yasukawa M 2000 Ferromagnetism in germanium clathrate: $Ba_8Mn_2Ge_{44}$ *Appl. Phys. Lett.* **77** 3438

[7] Li Y and Ross J H 2003 Ferromagnetism in Fe-doped Ba_6Ge_{25} chiral clathrate *Appl. Phys. Lett.* **83** 2868

[8] Woods G T, Martin J, Beekman M, Hermann R P, Grandjean F, Keppens V, Leupold O, Long G J and Nolas G S 2006 Magnetic and electronic properties of $Eu_4Sr_4Ga_{16}Ge_{30}$ *Phys. Rev.* B **73** 174403

[9] Phan M H, Woods G T, Chaturvedi A, Stefanoski S, Nolas G S and Srikanth H 2008 Long-range ferromagnetism and giant magnetocaloric effect in type VIII $Eu_8Ga_{16}Ge_{30}$ clathrates *Appl. Phys. Lett.* **93** 252505

[10] Guloy A M, Ramlau R, Tang Z, Schnelle W, Baitinger M and Grin Y 2006 A guest-free germanium clathrate *Nature* **443** 320

[11] Zhao J, Buldum A, Ping Lu J and Fong C Y 1999 Structural and electronic properties of germanium clathrates Ge_{46} and K_8Ge_{46} *Phys. Rev.* B **60** 14177

[12] Yang C-K, Zhao J and Lu J P 2004 Calculations of electronic structure of $Ge_{44}Mn_2Ba_8$ and $Ge_{42}Mn_4Ba_8$ clathrates *Phys. Rev.* B **70** 073201

[13] Kresse G and Furthmüller J 1996 Efficient iterative schemes for *ab initio* total-energy calculations using a plane-wave basis set *Phys. Rev.* B **54** 11169

[14] Kresse G and Hafner J 1993 *Ab initio* molecular dynamics for liquid metals *Phys. Rev.* B **47** 558

[15] Blöchl P E 1994 Projector augmented-wave method *Phys. Rev.* B **50** 17953

[16] Perdew J P, Burke K and Ernzerhof M 1996 Generalized gradient approximation made simple *Phys. Rev. Lett.* **77** 3865

[17] Dudarev S L, Botton G A, Savrasov S Y, Humphreys C J and Sutton A P 1998 Electron-energy-loss spectra and the structural stability of nickel oxide: an LSDA + U study *Phys. Rev.* B **57** 1505

[18] Ganguli N, Dasgupta I and Sanyal B 2009 The making of ferromagnetic Fe doped ZnO nanoclusters *Appl. Phys. Lett.* **94** 192503

[19] Dong J and Sankey O F 1999 Theoretical study of two expanded phases of crystalline germanium: clathrate-I and clathrate-II *J. Phys.: Condens. Matter* **11** 6129

[20] Saito S and Oshiyama A 1995 Electronic structure of Si_{46} and $Na_2Ba_6Si_{46}$ *Phys. Rev.* B **51** 2628

[21] Sarma D D, Mahadevan P, Saha-Dasgupta T, Ray S and Kumar A 2000 Electronic Structure of Sr_2FeMoO_6 *Phys. Rev. Lett.* **85** 2549

[22] Fang Z, Terakura K and Kanamori J 2001 Strong ferromagnetism and weak antiferromagnetism in double perovskites: Sr_2FeMO_6 (M = Mo, W, and Re) *Phys. Rev.* B **63** 180407

[23] Kanamori J and Terakura K 2001 A general mechanism underlying ferromagnetism in transition metal compounds *J. Phys. Soc. Japan* **70** 1433

[24] Mahadevan P, Zunger A and Sarma D D 2004 Unusual directional dependence of exchange energies in GaAs diluted with Mn: is the RKKY description relevant? *Phys. Rev. Lett.* **93** 177201

[25] Zhao Y-J, Shishidou T and Freeman A J 2003 Ruderman–Kittel–Kasuya–Yosida like ferromagnetism in Mn_xGe_{1-x} *Phys. Rev. Lett.* **90** 047204

[26] Matsukura F, Ohno H, Shen A and Sugawara Y 1998 Transport properties and origin of ferromagnetism in (Ga,Mn)As *Phys. Rev.* B **57** R2037